

TOWARDS INTERPRETING VISUAL INFORMATION PROCESSING IN VISION-LANGUAGE MODELS

Clement Neo^{1*}, Luke Ong¹, Philip Torr², Mor Geva³, David Krueger⁴, Fazl Barez^{2,5}

¹Nanyang Technological University ²University of Oxford ³Tel Aviv University

⁴MILA ⁵Tangentic

ABSTRACT

Vision-Language Models (VLMs) are powerful tools for processing and understanding text and images. We study the processing of visual tokens in the language model component of LLaVA, a prominent VLM. Our approach focuses on analyzing the localization of object information, the evolution of visual token representations across layers, and the mechanism of integrating visual information for predictions. Through ablation studies, we demonstrated that object identification accuracy drops by over 70% when object-specific tokens are removed. We observed that visual token representations become increasingly interpretable in the vocabulary space across layers, suggesting an alignment with textual tokens corresponding to image content. Finally, we found that the model extracts object information from these refined representations at the last token position for prediction, mirroring the process in text-only language models for factual association tasks. These findings provide crucial insights into how VLMs process and integrate visual information, bridging the gap between our understanding of language and vision models, and paving the way for more interpretable and controllable multimodal systems.

1 INTRODUCTION

Vision-Language Models (VLMs) take an image and text as input, and generate a text output. They have become powerful tools in processing and understanding text and images, enabling a wide range of applications from question answering to image captioning (Liu et al., 2023b; Li et al., 2023; Alayrac et al., 2022). Among VLM architectures, the “adapter” style has demonstrated impressive state-of-the-art performance, notable for its simplicity. These models combine a pre-trained image encoder, a pre-trained language model (LM), and a learned adapter network that maps image encoder outputs to soft prompts for LM inputs (Merullo et al., 2022; Liu et al., 2023b;a). Despite their importance and potential, the inner workings of VLMs remain poorly understood as compared to their text-only counterparts. While significant progress has been made in understanding language models (Elhage et al., 2021; Wang et al., 2023; Bricken et al., 2023) and, to a lesser extent, vision transformers (Palit et al., 2023; Vilas et al., 2023; Pan et al., 2024), there is a notable gap in our understanding of VLMs, where both modalities operate in the same space. A deeper comprehension of VLMs could lead to practical advances in safety, robustness, and functionality, similar to the progress made in language models, such as model editing (Meng et al., 2022) or identifying specific components responsible for certain behaviors (Arditi et al., 2024).

In this paper, we investigate the LM component of VLMs as they serve as the “brain” of the system, comprising more than 95% of the total parameters for models like LLaVA 1.5 7B. LLMs pre-trained on large text datasets are likely to remain the foundation of VLMs because of their powerful reasoning capabilities. Therefore, understanding how these LMs process and integrate visual information is crucial for advancing VLM interpretability.

Many open questions remain regarding the inner workings of VLMs. The nature and structure of visual representations fed into the LM remain unclear, as these visual inputs are soft prompts that

*Work done during ERA-Krueger AI Safety Lab internship.
Author contributions detailed in §6. Correspondence to Clement Neo <clement@clementneo.com>.

do not correspond to language tokens and cannot be interpreted as such (Lester et al., 2021; Merullo et al., 2022). This raises questions about how visual information is encoded in these representations. Furthermore, the spatial distribution of information within the image encoder’s feature maps remains unclear, leaving open the question of whether and how much object-specific details are localized or dispersed across the entire representation.

Furthermore, the mechanisms by which the language model processes these visual inputs are not well understood. A significant modality gap exists between visual and textual input (Jiang et al., 2024), and it is unclear whether our mechanistic understanding of text processing in language models generalizes to the processing of visual input in VLMs.

To understand the representations in the visual inputs for VLM and how the VLM processes them, we study LLaVA 1.5 7B (Liu et al., 2023a), a popular open-source VLM with competitive performance that uses CLIP (Radford et al., 2021) as an image encoder and Vicuna 13B (Chiang et al., 2023) as its language model. We also test on LLaVA-Phi¹ and Qwen2-VL (Wang et al., 2024). We focus on a set of object identification tasks and **our main contributions** are as follows:

1. Using ablation techniques, we demonstrate that the information for an object is highly localized to the token positions corresponding to their original location in the image.
2. By extending the *logit lens* technique primarily used for language models (Nostalgebraist, 2020), we find that the representations of the visual input in the LM are refined towards the embedding of interpretable tokens in the vocabulary, despite the LM not being explicitly trained to do so.
3. By blocking the attention flow between tokens, we show that the model extracts object information from the object tokens in the middle to late layers.

Our findings are first steps in understanding the internal mechanisms of VLMs, paving the way for more interpretable and controllable multimodal systems. The code for our experiments is available at <https://github.com/clemneo/llava-interp>.

2 BACKGROUND

Transformer Architecture. Transformer-based autoregressive Large Language Models (LLMs) process sequences of input tokens to predict the next token in the sequence (Vaswani et al., 2017). These models achieved state-of-the-art performance across various natural language processing tasks (Brown et al., 2020), even though they are merely trained on next-token prediction (Radford et al., 2019). A LLM takes an input sequence $X = (x_1, \dots, x_n)$ and outputs a probability distribution over the vocabulary V to predict the next token x_{n+1} .

To do so, the model refines token representations layer by layer through a series of computations. Each token x_i is initially represented by an embedding vector h_i^0 of dimension d_m , obtained from a lookup operation in an embedding matrix $W_E \in \mathbb{R}^{|V| \times d_m}$. This representation is then updated through successive layers using multi-head self-attention (MHSA) and feed-forward (FF) sublayers:

$$h_i^l = h_i^{l-1} + a_i^l + f_i^l \quad (1)$$

where h_i^l is the representation of token x_i at layer l , a_i^l is the output from the MHSA sublayer, and f_i^l is the output from the FF sublayer. All vectors $h_i^l, a_i^l, f_i^l \in \mathbb{R}^{d_m}$.

The MHSA sublayer consists of H attention heads working in parallel, each implemented as follows:

$$\text{Attention}(Q, K, V) = \text{softmax} \left(\frac{QK^T}{\sqrt{d_k}} + M \right) V \quad (2)$$

where $Q, K, V \in \mathbb{R}^{n \times d_k}$ are query, key, and value matrices derived from learned linear projections of the input, and $M \in \mathbb{R}^{n \times n}$ is a causal mask. The causal mask M is set to $-\infty$ in the upper right triangle, meaning $M_{ij} = 0$ if $i \geq j$, else $-\infty$. This ensures that each position can only attend to previous positions and itself, thus preserving the autoregressive property in language models. These

¹Sourced from the [xtuner HuggingFace model](#).

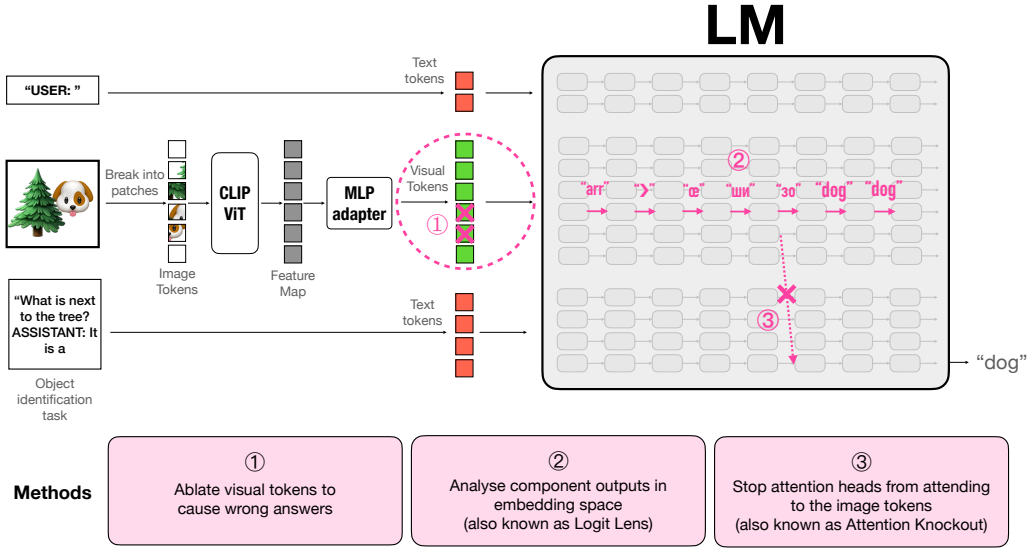


Figure 1: In adapter-style Vision-Language Models (VLMs), the visual tokens (in green) are soft prompts for the language model (LM), and are not interpretable through the vocabulary embedding. Through a set of object identification tasks, we find that (1) object information can be localized to a subset of visual tokens, (2) the representations of the visual tokens evolve towards interpretable text embeddings, and (3) the model extracts some information from the visual tokens to the last token position in the middle to late layers, to identify the object.

outputs are then concatenated and linearly projected to produce the final output of the multi-head attention sublayer.

The FF sublayer applies two linear transformations with an element-wise non-linear function σ between them:

$$f_i^l = W_v^l \sigma(W_k^l a_i^l + b_k^l) + b_v^l, \quad (3)$$

where W_v^l , W_k^l , b_k^l , and b_v^l are learned parameters. Finally, the representation of the last token x_n at the final layer, h_n^L , is projected into a probability distribution over V using an unembedding matrix $W_U \in \mathbb{R}^{d \times |V|}$ and a softmax operation.

Image Encoders. The transformer architecture has been successfully adapted for state-of-the-art image encoders, as demonstrated by [Dosovitskiy et al. \(2021\)](#). In this approach, input images are divided into fixed-size patches, flattened, and linearly embedded before being processed as a sequence of tokens, analogous to word embeddings in NLP tasks. Unlike text-based models, the attention mechanism in these image encoders is bidirectional (i.e., no masking is applied). The input sequence includes a special `class` token, whose final embedding is typically used for image classification tasks. The representations at the other token positions form what is called the *feature map* of the image.

Building upon this foundation, [Radford et al. \(2021\)](#) introduced Contrastive Language-Image Pre-training (CLIP), which jointly trains a vision transformer and a text transformer to produce similar embeddings for matching image-text pairs. CLIP’s image encoder is currently being used for state-of-the-art performance on many downstream tasks like zero-shot image classification and vision-language models like LLaVA.

Connecting Text and Image Models. [Tsimpoukelli et al. \(2021\)](#) pioneered the concept of training an image encoder such that its output can be used by a frozen language model for multimodal few-shot reasoning. [Merullo et al. \(2022\)](#) advanced this approach by freezing both the pre-trained image encoder and pre-trained language model, training only a linear map that converts image features into inputs for the text model. This introduced the “adapter style” approach, utilizing pre-trained components for both modalities.

Building on this foundation, Liu et al. (2023b) introduced LLaVA, which combined a CLIP ViT-L/14 image encoder with a Vicuna-13B language model, connected by a trained linear projection, or an MLP for improved performance (Liu et al., 2023a). Crucially, LLaVA’s training process focuses solely on fine-tuning for multimodal conversation, without any next-token pretraining on image-text pairs. This approach allows LLaVA to leverage the strong pre-trained capabilities of both the vision and language models while efficiently adapting to multimodal tasks.

2.1 NOTATION

In this section, we describe how an image and query is processed through LLaVA.

Image Processing. The input *image* I is processed by first being cropped into a square, then suitably resized before being divided into 576 image patches. The CLIP ViT-L/14 image encoder f_{CLIP} processes this image to produce a *feature map* $E_I = f_{\text{CLIP}}(I) \in \mathbb{R}^{N \times d_{\text{CLIP}}}$, where $N = 576$ is the number of image patches and d_{CLIP} is the dimensionality of CLIP’s embeddings. An *adapter network* A then maps these CLIP embeddings to the language model’s input space, yielding a set of *visual tokens* $E_A = A(E_I) \in \mathbb{R}^{N \times d}$, where d_m is the dimensionality of the language model’s input embeddings. We call E_A *visual tokens* to distinguish them from the image tokens.

Text Processing and Combined Input. For the text input, given a tokenized prompt sequence $T = (t_1, \dots, t_M)$, the embedding layer of the language model E_{LM} maps these tokens to embeddings: $E_T = E_{\text{LM}}(T) \in \mathbb{R}^{M \times d_{\text{LM}}}$. The full input to the language model is the concatenation of the adapted image embeddings and the text embeddings: $X = [E_A; E_T] \in \mathbb{R}^{(N+M) \times d_{\text{LM}}}$, from which the language model can generate output autoregressively.

2.2 OPEN QUESTIONS AND HYPOTHESES

One might expect that the output of the adapter E_A would produce embeddings corresponding to image information. For example, if the image contained a car, we might expect the adapter to produce tokens that correspond to the embedding of “car”. However, the output of the adapter forms soft prompts that have no semantic meaning when decoded through the vocabulary (Merullo et al., 2022; Bailey et al., 2023).

2.2.1 LOCALIZATION OF OBJECT-SPECIFIC INFORMATION

A key question of our investigation is: **Where is object-specific information located in visual tokens?** Two conflicting hypotheses emerge from recent research:

1. **Object-Centric Localization:** Joseph & Nanda (2024) found that in classical vision transformers, token representations corresponding to specific object locations tended to align with those objects’ class embeddings in the late layers, even without explicitly training for this behavior. This suggest that object information might be localized to the tokens corresponding to the spatial location of the object in the original image. However, their findings were on a vision transformer trained on ImageNet classes, and not the vision transformer in CLIP.
2. **Global Information in Register Tokens:** In contrast, Darcet et al. (2024) identified *register tokens* in vision transformers, including a CLIP variant. These are background patch tokens with unusually high norms that appear to encode global image features. It follows that the LM in an adapter-style VLM could primarily rely on these information-rich register tokens for its output.

We investigate these hypotheses in Section 3 using ablation techniques in a set of object identification tasks.

2.2.2 PROCESSING OF OBJECT-SPECIFIC REPRESENTATION

The processing of visual tokens may differ from text tokens. Soft prompts are very different from normal prompts (Bailey et al., 2023), and there is a *modality gap* between textual and visual representations in VLMs (Jiang et al., 2024). Furthermore, LLaVA is fine-tuned exclusively on visual question-answering (VQA) prompt-response pairs, without pre-training on next-token prediction.

This may affect how the model processes visual information as compared to text. In Section 4.1, we attempt the *logit lens* method to see how the representations of visual tokens evolve through the layers.

Recent studies have shed light on how LMs process information. Geva et al. (2023) identified a refine-then-extract process in factual association prompts, where the model first refines information at subject tokens through MLP sublayers before transferring it to the last token position via attention sublayers. Similar mechanisms have been observed in arithmetic tasks (Stolfo et al., 2023), suggesting that this (sequencing of functions) might be a general mechanism in LMs.

However, Basu et al. (2024) adapted the factual association setup to VLMs and found preliminary evidence that the LM may first summarize image information in text tokens, instead of extracting the image information to the last token position from the image tokens directly. While we do not study factual association – rather we choose to focus on a simpler object identification task, we study how information flows from the image tokens in Section 4.2.

3 INVESTIGATING THE REPRESENTATIONS IN MAPPED VISUAL TOKENS

In this section, we use ablation experiments to test if object information is concentrated in specific visual tokens. By ablating selected tokens and observing degradations in the model’s ability to identify the object, we map how object information is distributed across the visual tokens.

Dataset. We use images from the COCO Detection Training set (Lin et al., 2014). To ensure the reliability of our results, we employ two filtering steps:

(1) *Choosing Simpler Images.* As a heuristic to focus on simpler images, we choose images where (a) there is an object whose size is between 1,000-2,000 square pixels, or about 2-4% of the image by area, (b) only one instance of the that object is present in the image, and (c) there are less than 4 annotated objects. We present a few examples of the images in Figure 4.

(2) *Controlling for Hallucination.* Model can sometimes hallucinate objects based on context, even when the object’s visual information is removed. To address this, we create two versions of each image: the original and one where the target object is masked with noise. We only keep images where the model correctly identifies the object in the original image but fails to identify it in the masked version. This ensures that the model’s object identification relies on the object’s visual information.

After applying both filtering steps, our final dataset comprises 4,318 images.

Method. We present a high level overview of our methodology in Figure 2. Let $E_A = \{e_1, \dots, e_N\}$ be the set of visual tokens. We define a subset $S \subset \{1, \dots, N\}$ consisting of the indices of tokens hypothesized to contain information about a particular object o in the image.

For each ablation experiment, we create a modified set of embeddings E'_A :

$$e'_i = \begin{cases} \bar{e} & \text{if } i \in S \\ e_i & \text{otherwise} \end{cases}$$

where $\bar{e} = \frac{1}{N} \sum_{i=1}^N e_i$ is the mean embedding across all visual tokens from 50,000 images from the ImageNet validation split (Deng et al., 2009). This replaces the hypothesized object-relevant tokens with an average token, effectively ablating their specific information. We do mean ablation to preserve the norm of the image token and keep them in-distribution, as their norms are typically much higher than the norm of text tokens (Bailey et al., 2023). We then evaluate the impact of token ablation using three methods:

1. **Generative Description:** We prompt the model with “Describe the image” using both the original (E_A) and ablated embeddings (E'_A). We then ascertain whether the target object o is produced verbatim in the model’s generated description before and after ablation. If o is mentioned with E_A and not E'_A , it indicates that the ablated tokens were crucial for the model to identify and include the object in its description.
2. **Binary Polling:** We ask the model “Is there a [o] in this image?” using both E_A and E'_A . We then compare whether the model’s next generated token changes from “Yes” to

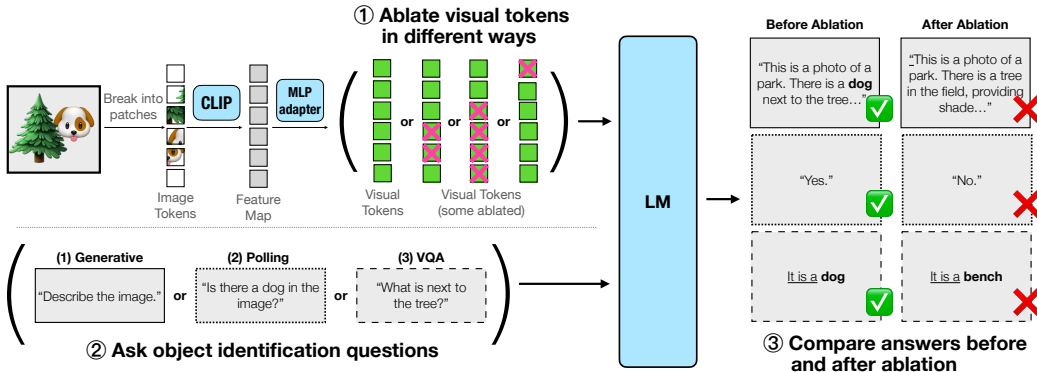


Figure 2: Overview of our ablation experiments. (1) We ablate some visual tokens that potentially contain object-specific information, (2) prompt the model to describe the image, or answer object-specific questions, then (3) measure the impact of token ablation by calculating the percentage of initially correct object identifications that become incorrect after ablation.

“No” after ablation, which indicates that the ablated tokens were crucial for identifying the object.

3. **Visual Question-Answering:** We manually curate a set of 100 images with specific questions about objects, such as “What is on the bed?”. We choose questions with unambiguous answers and avoid objects directly related to the question (e.g., avoiding “pillow” for a bed-related question). We prefill the model’s response with “It is a” and compare the next generated token before and after ablation. A set of examples is in Figure 5.

We choose the subset S of tokens to ablate in five ways:

- (1) *Object Tokens.* We choose the visual tokens whose positions correspond to the image patches that originally contained that object.
- (2) *Object Tokens with Buffer.* In addition to the object tokens, we include neighboring tokens. We test with two buffer sizes: 1 Buffer (including immediately adjacent tokens) and 2 Buffer (including tokens up to 2 positions away from object tokens).
- (3) *Register Tokens.* We select visual tokens with norms more than 2 standard deviations from the mean norm. These correspond to the register tokens identified by [Darcet et al. \(2024\)](#), which are thought to encode global image features.
- (4) *Random Tokens.* As a baseline, we ablate n random tokens.
- (5) *High-Gradient Tokens.* As a stronger baseline, we use the Integrated Gradients attribution method ([Sundararajan et al., 2017](#)) to identify tokens most important for the model’s decision. For a given object o , we prompt the model with “Is there a [o] in the image?” and compute integrated gradients with respect to the logit for the “Yes” token over 50 steps. We then ablate the n tokens with the highest attribution scores.

Results. Our results are presented in Table 1. We find that ablating the object tokens significantly impairs the model’s ability to identify the object. For comparable numbers of ablated tokens, object token ablation consistently results in larger performance decreases across all settings as compared to the gradient-based and random baselines. This suggests that the information about that object is localised to the region of the object token. Furthermore, these findings are consistent across all three experimental settings and applicable to both LLaVA 1.5 and LLaVA-Phi.

4 INVESTIGATING VISUAL INFORMATION PROCESSING

4.1 ANALYZING THE RESIDUAL STREAM THROUGH EMBEDDING SPACE

Can we interpret how the representations at the visual token positions evolve through the layers? To do so, we employ the *logit lens* technique ([Nostalgebraist, 2020](#)): for each layer, we decode the activation at each token position using the unembedding. Formally, for each hidden state h_i^l at each token position i and layer l , we project it into a probability distribution over V using W_U and take the token with the highest logit. We do this for LLaVA 1.5.

Table 1: **Performance degradation after token ablation.** A lower percentage indicates a greater impact of the ablation, meaning the model is more likely to answer incorrectly, thus suggesting that the ablated tokens contain more localized object information. Average token counts apply to both the generative and polling settings for LLaVA 1.5. We find that ablating the object tokens with adjacent tokens (33.4 tokens on average, in **bold**) significantly causes object identification performance to drop, more so than the integrated gradients and random baselines for a comparable number of tokens (40 tokens, in **bold**).

Ablation Type (Avg Token Count)	LLaVA 1.5			LLaVA-Phi		
	Generative Decrease (%)	Polling Decrease (%)	VQA Decrease (%)	Generative Decrease (%)	Polling Decrease (%)	VQA Decrease (%)
Object (12.6)	33.33	15.38	33.33	47.46	28.48	41.51
+ 1 Buffer (33.4)	71.79	51.28	86.67	82.89	86.48	96.23
+ 2 Buffer (60)	76.92	64.10	92.22	89.56	95.49	100.00
Register tokens (3.1)	5.13	0.00	3.33	7.63	0.00	1.89
Int. Gradients (5)	2.56	0.00	6.67	17.11	1.23	28.30
Int. Gradients (10)	20.51	2.56	6.67	25.26	4.30	24.53
Int. Gradients (20)	33.33	20.51	17.78	41.14	9.63	37.74
Int. Gradients (40)	48.72	35.90	50.00	61.49	26.64	56.60
Int. Gradients (60)	58.97	48.72	71.11	70.61	40.98	69.81
Int. Gradients (100)	76.92	51.28	84.44	81.23	61.68	83.02
Int. Gradients (250)	76.92	69.23	97.78	91.93	90.16	98.11
Random (5)	0.00	0.00	1.11	3.68	0.00	0.00
Random (10)	4.88	0.00	0.00	3.95	0.00	1.89
Random (20)	2.44	0.00	2.22	5.88	0.00	0.00
Random (40)	2.44	0.00	0.00	8.51	0.00	0.00
Random (60)	7.32	0.00	1.11	9.39	0.41	3.77
Random (100)	7.32	0.00	4.44	11.23	0.20	7.55
Random (250)	24.39	0.00	16.67	20.61	1.84	15.09

Results. We find that the activations in the late layers at each visual token position correspond to token embeddings that describe its original patch object in its corresponding image token. We provide some case studies in Figure 3, and an [interactive demo](#) on more examples.

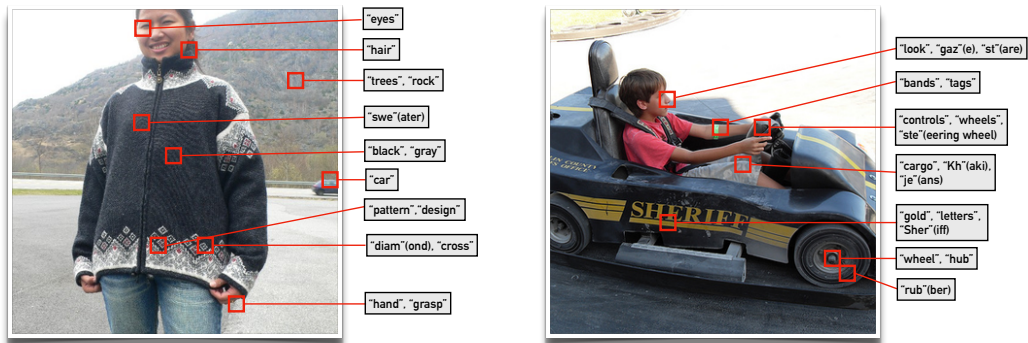
To quantify this phenomenon, we analyzed 170 COCO validation images with objects of sizes between 20,000 and 30,000 square pixels (approximately 1/2 width and 1/3 height of the image). We found that in the best-performing layer for each image, an average of 23.7% of the object patch token positions correspond to the correct object class token. The best-performing layer occurs on average at layer 25.7 (out of 33 layers), confirming that mid-to-late layers tend to develop the strongest object-token correspondences (Figure 6).

We found that the tokens decoded often correspond to concepts more specific than the object-level. For example, in Figure 3a, the tokens go beyond identifying the sweater worn (“swe”) and describe the specific patterns on the sweater with tokens like “diam”(ond) and “cross”.

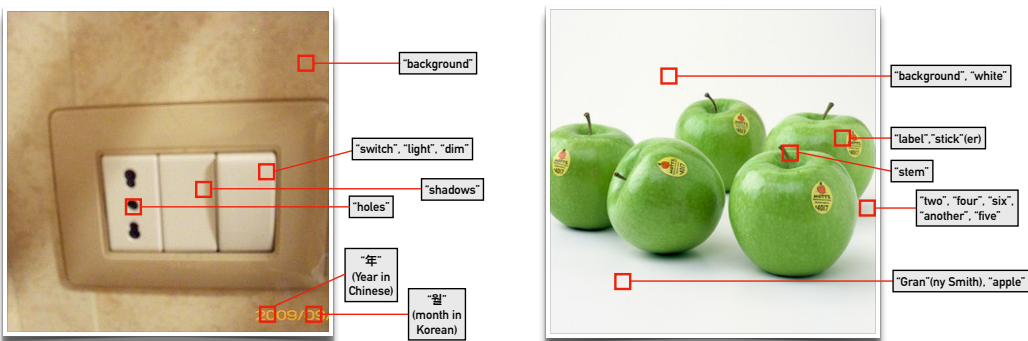
In some instances, tokens correspond to their corresponding concepts in other languages, like in Figure 3c where the tokens correspond to “year” and “month” but in Chinese and Korean instead. This is somewhat surprising given that previous work has shown that Llama used for non-English languages tend to have English tokens in their intermediate activations when interpreted through the logit lens (Wendler et al., 2024).

Overall, it is surprising that the logit lens work on VLMs! This technique works on auto-regressive LLMs because they are *pretrained on next-token prediction*, meaning their activations will be iteratively refined towards the unembedding of the predicted next token. However, VLMs are merely fine-tuned on multimodal tasks. The effectiveness of the logit lens here suggests that the hypothesis that transformers build predictions by promoting concepts in vocabulary space (Geva et al., 2022) may generalise to VLMs, even when only fine-tuned on multimodal tasks.

Testing Other Models. We extended our logit lens analysis to Qwen2VL-2B to verify if these findings generalize beyond the LLaVA family. Following the same methodology, we analyzed 253 COCO validation images and found that in the best-performing layer, an average of 6.5% of the visual tokens map to the correct object class token. The best-performing layer occurs at layer 25.1 (out of 29 layers), confirming the middle-to-late layer pattern observed in LLaVA (Figure 7). Inter-



(a) An image of a lady in the sweater. The logit lens identifies tokens that correspond to specific detail of the sweater, such as “pattern” and “diam”(ond). (b) An image of a child in a go-kart. The representations sometimes encode specific details, such as “look” and “gaz”(e) instead of just “face”.



(c) An image of a switch. In the intermediate layers, the year and month tokens are encoded in non-English characters. (d) An image of a bunch of apples. Global features, like count, show up in background tokens, though this may be an artifact of the LM processing.

Figure 3: Examples of tokens and their positions that the logit lens yields in the late layers. The labelled tokens come from a range of layers around the middle-to-late layers. In our labelling for an image, tokens that are part of a word are completed with an educated guess e.g. “diam”(ond)

estingly, Qwen2VL shows non-zero correspondence even in early layers, possibly due to its cross-attention adapter providing better initial mapping compared to LLaVA’s simpler MLP adapter. Both models demonstrate increasingly aligned token representations with object tokens in later layers, suggesting this refinement pattern is a general property of adapter-style VLMs.

Case Study: Global Features. We sometimes find global-level features, such as numbers possibly referring to object counts, appearing in unexpected background tokens (Figure 3d). Ablating these specific tokens doesn’t change the model’s description, and the numbers persist in the logit lens even after ablation. This suggests these global features may be artifacts of the language model’s processing rather than direct information from visual tokens—potentially explaining why CLIP-based VLMs often underperform CLIP itself on classification tasks (Zhang et al., 2024).

Potential Applications. This may be useful for getting coarse segmentation maps for little to no extra computation, which could lead to downstream applications. For example, Liu et al. (2024) suggests to adjust the attention weights towards the visual tokens in the LM to reduce hallucinations. We speculate that directing attention towards specific objects may improve this method, though we leave further exploration to future work.

4.2 TRACING ATTENTION FLOW

To understand how visual information is processed and integrated within the language model, we investigate the flow of critical information through the network. Specifically, we examine whether the

model directly extracts information from relevant visual tokens, or whether it aggregates information from visual tokens before transferring it to the final output token.

Method. We employ the *attention knockout* technique introduced by Geva et al. (2023). This method involves selectively blocking attention between specific tokens at different layers of the model, allowing us to assess the importance of various connections for the model to identify the object. Our process is as follows:

(1) For a given input and target layer ℓ , we artificially block specific attention connections in the multi-head self-attention (MHSA) sublayer by setting the corresponding attention mask values to negative infinity: $M_{rc}^{\ell+1,j} = -\infty \quad \forall j \in [1, H]$ where $M^{\ell+1,j}$ is the attention mask for head j at layer $\ell + 1$, and r and c are the indices of the tokens between which we want to block attention.

(2) We apply this blocking over a window of consecutive layers, including early layers (L1-10), early to middle layers (L5-14), middle layers (L11-20), middle to late layers (L15-24), and late layers (L21-31).

(3) For each window, we measure the decrease in accuracy and prediction probability for the correct token when blocking attention under three scenarios: (i) From object tokens and their surrounding buffer to the final token. (ii) From all non-object tokens to the final token. (iii) From all visual tokens except the last row to the last row of visual tokens².

We conduct this experiment using LLaVA 1.5 on our curated Visual Question Answering (VQA) dataset of 100 images.

Findings. Our results are presented in Table 2.

We find that blocking attention from the object tokens (and their buffers) to the final token in mid-late layers leads to noticeable performance degradation. This suggests that the model directly extracts object-specific information in these later stages. Blocking attention from non-object tokens to the final token in early layers also causes some performance drop. This indicates that contextual information from the broader image is processed and integrated in the earlier stages of the model.

Interestingly, blocking attention from visual tokens to the last row of visual tokens has minimal effect on performance. This contrasts with findings by Basu et al. (2024), who suggested that the model might summarize image information in the last row of visual tokens before using it. Our results indicate that, at least for our object identification tasks, the model doesn’t rely on such a summarization step.

Table 2: Results of blocking attention between different token groups across various layers of the LLaVA 1.5 model. The values represent the relative performance on the correct token being predicted when blocking attention, with 1.00 being no impact and 0.00 being all questions wrong post-ablation.

Attention Blocking		Layer					
From*	To†	Early	Early-Mid	Mid	Mid-Late	Late	All
O	LTP	1.00	1.00	0.96	0.88	0.93	0.82
O+1	LTP	1.00	0.99	0.90	0.82	0.89	0.67
O+2	LTP	1.00	1.00	0.91	0.80	0.91	0.68
I-(O+1)	LTP	0.88	1.00	0.97	0.96	0.98	0.82
O+1	LVR	1.00	1.00	1.00	1.00	1.00	1.00
I-LVR	LVR	1.00	1.00	1.00	1.00	1.00	1.00

*From: O = Object Tokens, O+n = O + n Buffer,

I-(O+1) = All visual tokens except O+1, I-LVR = All visual tokens except last row

†To: LTP = Last Token Position, LVR = Last Visual Token Row

²We do this as recent work by Basu et al. (2024) suggests that the model may summarise visual information in the last row of visual tokens, though they study this in a different VQA task. If the model does use the last row of visual tokens as a ‘working summary’, then blocking the attention from all the visual tokens to the last row should prevent it from answering the question.

Testing Other Models. To verify that our attention blocking results are not specific to LLaVA-1.5, we conducted additional experiments with LLaVA-Phi-3. Rather than using fixed layer groupings, we employed a sliding window of 10 layers to obtain finer-grained results across the network. We find that the results (Figure 8) closely mirror our original results: blocking attention from object tokens to the last token position shows the strongest effect in middle-to-late layers, while blocking attention from visual tokens to the last row continues to show minimal impact.

5 RELATED WORK

Explainability. Classical techniques like GRAD-Cam (Selvaraju et al., 2017) and Integrated Gradients (Sundararajan et al., 2017), focus on input attribution, while recent tools like LVLM-Interpret (Stan et al., 2024) extend these methods to VLMs. Our work complements these by investigating the model’s internal processing mechanisms.

Mechanistic Interpretability (MI) for LLMs. Techniques such as causal tracing (Meng et al., 2022) and sparse coding (Bricken et al., 2023; Huben et al., 2023; Marks et al., 2024) have advanced our understanding of how LLMs perform tasks despite being primarily trained for next-token prediction, but VLMs are not trained on next-token prediction for visual inputs (Liu et al., 2023b). Our work extends some of these techniques to understand visual information processing in multimodal contexts.

MI for Multimodal Models. In CLIP, researchers have discovered multimodal neurons (Goh et al., 2021), decomposed image representations (Gandelsman et al., 2023; 2024), identified interpretable network subgraphs (Rajaram et al., 2024), and extracted interpretable features using sparse coding (Rao et al., 2024; Daujotas, 2024; Fry, 2024). In contrast, our work focuses on generative VLMs.

For generative VLMs, Schwettmann et al. (2023) found neurons corresponding to visual concepts, while Palit et al. (2023) adapted causal tracing for BLIP. While these studies help us understand the role of specific components in the VLM, we investigate the representations of the visual inputs.

Basu et al. (2024) used causal tracing and attention contributions in a visual question-answering setup to find that VLMs such as LLaVA retrieve information from earlier causal layers of the LLM (i.e. layers 1-4 vs layers 4-7 in an LLM) when answering a multi-modal question. Their analysis suggests that the visual information may be summarised in a consistent subset of late visual tokens. In contrast, we study VLMs in a more straightforward object-identification setting. We also examine their information transfer hypothesis through our attention blocking experiments in Section 4.2.

Parallel Work. Concurrent research by Jiang et al. (2025) independently arrived at similar logit lens findings and developed a hallucination reduction method based on these insights. Wu et al. (2024) observed comparable logit lens patterns across both visual and audio modalities.

6 CONCLUSION

Our investigation into visual information processing in LLaVA reveals that object information is highly localized within visual tokens corresponding to the object’s spatial location, challenging the hypothesis that VLMs primarily rely on global features in register tokens. Visual token representations evolve to align with interpretable textual concepts across layers, suggesting VLMs refine visual information toward language-like representations even without next-token prediction pretraining for visual inputs. Our attention blocking experiments suggest that VLMs may extract object information from relevant visual tokens in mid-to-late layers. These findings bridge the gap between our understanding of language and vision models, providing a foundation for more interpretable multimodal systems.

Limitations & Future Work. We focused on LLaVA-type models as a starting point for interpreting more complex VLMs, but our results may not generalize to significantly different architectures. Our study concentrates on object identification tasks, providing a simpler setup compared to multi-step reasoning. While we tested object identification in three ways, our findings may not fully represent VLM behavior in complex tasks like reasoning or open-ended question answering. Future work should explore practical applications in reducing hallucinations and enhancing factual accuracy, while examining whether these findings extend to broader task types and model architectures.

AUTHOR CONTRIBUTIONS

Clement Neo conceived the study, designed and performed the experiments, and led the writing of the manuscript. Luke Ong contributed to the writing and literature review. Philip Torr, Mor Geva and David Krueger provided advice and comments. Fazl Barez served as the primary advisor for this work and helped significantly with the design and write-up of the paper.

ACKNOWLEDGMENTS

We thank the Torr Vision Group for providing compute and hosting Clement Neo during the internship.

We thank Sarah Schwettmann, Ashkan Khakzar, William Rudman, Joseph Miller, Alex Spies for discussing and reading drafts of the paper.

REFERENCES

- Jean-Baptiste Alayrac, Jeff Donahue, Pauline Luc, Antoine Miech, Iain Barr, Yana Hasson, Karel Lenc, Arthur Mensch, Katherine Millican, Malcolm Reynolds, et al. Flamingo: a visual language model for few-shot learning. *Advances in neural information processing systems*, 35:23716–23736, 2022.
- Andy Arditi, Oscar Obeso, Aaqib Syed, Daniel Paleka, Nina Panickssery, Wes Gurnee, and Neel Nanda. Refusal in language models is mediated by a single direction, 2024. URL <https://arxiv.org/abs/2406.11717>.
- Luke Bailey, Gustaf Ahdriz, Anat Kleiman, Siddharth Swaroop, Finale Doshi-Velez, and Weiwei Pan. Soft prompting might be a bug, not a feature. 2023.
- Samyadeep Basu, Martin Grayson, Cecily Morrison, Besmira Nushi, Soheil Feizi, and Daniela Mas-siceti. Understanding Information Storage and Transfer in Multi-modal Large Language Models, jun 2024. URL <http://arxiv.org/abs/2406.04236>.
- Trenton Bricken, Adly Templeton, Joshua Batson, Brian Chen, Adam Jermyn, Tom Con-erly, Nick Turner, Cem Anil, Carson Denison, Amanda Askell, Robert Lasenby, Yifan Wu, Shauna Kravec, Nicholas Schiefer, Tim Maxwell, Nicholas Joseph, Zac Hatfield-Dodds, Alex Tamkin, Karina Nguyen, Brayden McLean, Josiah E Burke, Tristan Hume, Shan Carter, Tom Henighan, and Christopher Olah. Towards monosemanticity: Decomposing language models with dictionary learning. *Transformer Circuits Thread*, 2023. <https://transformer-circuits.pub/2023/monosemantic-features/index.html>.
- Tom Brown, Benjamin Mann, Nick Ryder, Melanie Subbiah, Jared D Kaplan, Prafulla Dhari-wal, Arvind Neelakantan, Pranav Shyam, Girish Sastry, Amanda Askell, Sandhini Agar-wal, Ariel Herbert-Voss, Gretchen Krueger, Tom Henighan, Rewon Child, Aditya Ramesh, Daniel Ziegler, Jeffrey Wu, Clemens Winter, Chris Hesse, Mark Chen, Eric Sigler, Mateusz Litwin, Scott Gray, Benjamin Chess, Jack Clark, Christopher Berner, Sam McCandlish, Alec Radford, Ilya Sutskever, and Dario Amodei. Language models are few-shot learners. In H. Larochelle, M. Ranzato, R. Hadsell, M.F. Balcan, and H. Lin (eds.), *Advances in Neu-ral Information Processing Systems*, volume 33, pp. 1877–1901. Curran Associates, Inc., 2020. URL https://proceedings.neurips.cc/paper_files/paper/2020/file/1457c0d6bfcb4967418bfb8ac142f64a-Paper.pdf.
- Wei-Lin Chiang, Zhuohan Li, Zi Lin, Ying Sheng, Zhanghao Wu, Hao Zhang, Lianmin Zheng, Siyuan Zhuang, Yonghao Zhuang, Joseph E Gonzalez, et al. Vicuna: An open-source chatbot impressing gpt-4 with 90%* chatgpt quality. See <https://vicuna.lmsys.org> (accessed 14 April 2023), 2(3):6, 2023.
- Timothée Darcet, Maxime Oquab, Julien Mairal, and Piotr Bojanowski. Vision transformers need registers. In *The Twelfth International Conference on Learning Representations*, 2024.

- Gytis Daujotas. Case study: Interpreting, manipulating, and controlling clip with sparse autoencoders, 2024. URL <https://www.lesswrong.com/posts/iYFuZo9BMvr6GgMs5/case-study-interpreting-manipulating-and-controlling-clip>. Accessed: 2024-09-24.
- Jia Deng, Wei Dong, Richard Socher, Li-Jia Li, Kai Li, and Li Fei-Fei. Imagenet: A large-scale hierarchical image database. In *2009 IEEE Conference on Computer Vision and Pattern Recognition*, pp. 248–255, 2009. doi: 10.1109/CVPR.2009.5206848.
- Alexey Dosovitskiy, Lucas Beyer, Alexander Kolesnikov, Dirk Weissenborn, Xiaohua Zhai, Thomas Unterthiner, Mostafa Dehghani, Matthias Minderer, Georg Heigold, Sylvain Gelly, Jakob Uszkoreit, and Neil Houlsby. An image is worth 16x16 words: Transformers for image recognition at scale. In *International Conference on Learning Representations*, 2021. URL <https://openreview.net/forum?id=YicbFdNTTy>.
- Nelson Elhage, Neel Nanda, Catherine Olsson, Tom Henighan, Nicholas Joseph, Ben Mann, Amanda Askell, Yuntao Bai, Anna Chen, Tom Conerly, Nova DasSarma, Dawn Drain, Deep Ganguli, Zac Hatfield-Dodds, Danny Hernandez, Andy Jones, Jackson Kernion, Liane Lovitt, Kamal Ndousse, Dario Amodei, Tom Brown, Jack Clark, Jared Kaplan, Sam McCandlish, and Chris Olah. A mathematical framework for transformer circuits. *Transformer Circuits Thread*, 2021. <https://transformer-circuits.pub/2021/framework/index.html>.
- Hugo Fry. Towards multimodal interpretability: Learning sparse interpretable features in vision transformers, 2024. URL https://www.lesswrong.com/posts/bCtbuWraqYTDtuARg/towards-multimodal-interpretability-learning-sparse-2#Future_Work. Accessed: 2024-06-28.
- Yossi Gandelsman, Alexei A. Efros, and Jacob Steinhardt. Interpreting clip’s image representation via text-based decomposition, 2023.
- Yossi Gandelsman, Alexei A. Efros, and Jacob Steinhardt. Interpreting the second-order effects of neurons in clip, 2024.
- Mor Geva, Avi Caciularu, Kevin Wang, and Yoav Goldberg. Transformer feed-forward layers build predictions by promoting concepts in the vocabulary space. In *Proceedings of the 2022 Conference on Empirical Methods in Natural Language Processing*, pp. 30–45, 2022.
- Mor Geva, Jasmijn Bastings, Katja Filippova, and Amir Globerson. Dissecting recall of factual associations in auto-regressive language models. In *Proceedings of the 2023 Conference on Empirical Methods in Natural Language Processing*, pp. 12216–12235, 2023.
- Gabriel Goh, Nick Cammarata †, Chelsea Voss †, Shan Carter, Michael Petrov, Ludwig Schubert, Alec Radford, and Chris Olah. Multimodal neurons in artificial neural networks. *Distill*, 2021. doi: 10.23915/distill.00030. <https://distill.pub/2021/multimodal-neurons>.
- Robert Huben, Hoagy Cunningham, Logan Riggs Smith, Aidan Ewart, and Lee Sharkey. Sparse autoencoders find highly interpretable features in language models. In *The Twelfth International Conference on Learning Representations*, 2023.
- Chaoya Jiang, Haiyang Xu, Mengfan Dong, Jiaying Chen, Wei Ye, Ming Yan, Qinghao Ye, Ji Zhang, Fei Huang, and Shikun Zhang. Hallucination augmented contrastive learning for multimodal large language model, 2024. URL <https://arxiv.org/abs/2312.06968>.
- Nick Jiang, Anish Kachinthaya, Suzie Petryk, and Yossi Gandelsman. Interpreting and editing vision-language representations to mitigate hallucinations, 2025. URL <https://arxiv.org/abs/2410.02762>.
- Sonia Joseph and Neel Nanda. Laying the foundations for vision and multimodal mechanistic interpretability & open problems, 2024. URL <https://www.alignmentforum.org/posts/kobJymvvcvbjWfKe/laying-the-foundations-for-vision-and-multimodal-mechanistic>. Accessed: 2024-06-28.

- Brian Lester, Rami Al-Rfou, and Noah Constant. The power of scale for parameter-efficient prompt tuning. In Marie-Francine Moens, Xuanjing Huang, Lucia Specia, and Scott Wen-tau Yih (eds.), *Proceedings of the 2021 Conference on Empirical Methods in Natural Language Processing*, pp. 3045–3059, Online and Punta Cana, Dominican Republic, November 2021. Association for Computational Linguistics. doi: 10.18653/v1/2021.emnlp-main.243. URL <https://aclanthology.org/2021.emnlp-main.243>.
- Junnan Li, Dongxu Li, Silvio Savarese, and Steven Hoi. Blip-2: Bootstrapping language-image pre-training with frozen image encoders and large language models. In *International conference on machine learning*, pp. 19730–19742. PMLR, 2023.
- Tsung-Yi Lin, Michael Maire, Serge Belongie, James Hays, Pietro Perona, Deva Ramanan, Piotr Dollár, and C Lawrence Zitnick. Microsoft coco: Common objects in context. In *Computer Vision—ECCV 2014: 13th European Conference, Zurich, Switzerland, September 6–12, 2014, Proceedings, Part V 13*, pp. 740–755. Springer, 2014.
- Haotian Liu, Chunyuan Li, Yuheng Li, and Yong Jae Lee. Improved baselines with visual instruction tuning, 2023a.
- Haotian Liu, Chunyuan Li, Qingyang Wu, and Yong Jae Lee. Visual instruction tuning. In *NeurIPS*, 2023b.
- Shi Liu, Kecheng Zheng, and Wei Chen. Paying more attention to image: A training-free method for alleviating hallucination in vlms, 2024. URL <https://arxiv.org/abs/2407.21771>.
- Samuel Marks, Can Rager, Eric J Michaud, Yonatan Belinkov, David Bau, and Aaron Mueller. Sparse feature circuits: Discovering and editing interpretable causal graphs in language models. *arXiv preprint arXiv:2403.19647*, 2024.
- Kevin Meng, David Bau, Alex Andonian, and Yonatan Belinkov. Locating and editing factual associations in GPT. *Advances in Neural Information Processing Systems*, 36, 2022. arXiv:2202.05262.
- Jack Merullo, Louis Castricato, Carsten Eickhoff, and Ellie Pavlick. Linearly mapping from image to text space. In *The Eleventh International Conference on Learning Representations*, 2022.
- Nostalgebraist. Interpreting gpt: The logit lens. <https://www.alignmentforum.org/posts/AcKRB8wDpdaN6v6ru/interpreting-gpt-the-logit-lens>, Aug 2020. Accessed: 23 Sep 2024.
- Vedant Palit, Rohan Pandey, Aryaman Arora, and Paul Pu Liang. Towards vision-language mechanistic interpretability: A causal tracing tool for blip. In *Proceedings of the IEEE/CVF International Conference on Computer Vision*, pp. 2856–2861, 2023.
- Xu Pan, Aaron Philip, Ziqian Xie, and Odelia Schwartz. Dissecting query-key interaction in vision transformers. *ICML MI Workshop*, 2024.
- Alec Radford, Jeffrey Wu, Rewon Child, David Luan, Dario Amodei, Ilya Sutskever, et al. Language models are unsupervised multitask learners. *OpenAI blog*, 1(8):9, 2019.
- Alec Radford, Jong Wook Kim, Chris Hallacy, Aditya Ramesh, Gabriel Goh, Sandhini Agarwal, Girish Sastry, Amanda Askell, Pamela Mishkin, Jack Clark, Gretchen Krueger, and Ilya Sutskever. Learning transferable visual models from natural language supervision, 2021. URL <https://arxiv.org/abs/2103.00020>.
- Achyuta Rajaram, Neil Chowdhury, Antonio Torralba, Jacob Andreas, and Sarah Schwettmann. Automatic discovery of visual circuits, 2024. URL <https://arxiv.org/abs/2404.14349>.
- Sukrut Rao, Sweta Mahajan, Moritz Böhle, and Bernt Schiele. Discover-then-name: Task-agnostic concept bottlenecks via automated concept discovery, 2024. URL <https://arxiv.org/abs/2407.14499>.
- Sarah Schwettmann, Neil Chowdhury, Samuel Klein, David Bau, and Antonio Torralba. Multimodal neurons in pretrained text-only transformers. In *Proceedings of the IEEE/CVF International Conference on Computer Vision*, pp. 2862–2867, 2023.

- Ramprasaath R Selvaraju, Michael Cogswell, Abhishek Das, Ramakrishna Vedantam, Devi Parikh, and Dhruv Batra. Grad-cam: Visual explanations from deep networks via gradient-based localization. In *Proceedings of the IEEE international conference on computer vision*, pp. 618–626, 2017.
- Gabriela Ben Melech Stan, Estelle Aflalo, Raanan Yehezkel Rohekar, Anahita Bhiwandiwalla, Shao-Yen Tseng, Matthew Lyle Olson, Yaniv Gurwicz, Chenfei Wu, Nan Duan, and Vasudev Lal. Lvlm-intrepret: An interpretability tool for large vision-language models. In *Proceedings of the IEEE/CVF Conference on Computer Vision and Pattern Recognition*, pp. 8182–8187, 2024.
- Alessandro Stolfo, Yonatan Belinkov, and Mrinmaya Sachan. A mechanistic interpretation of arithmetic reasoning in language models using causal mediation analysis. In *Proceedings of the 2023 Conference on Empirical Methods in Natural Language Processing*, pp. 7035–7052, 2023.
- Mukund Sundararajan, Ankur Taly, and Qiqi Yan. Axiomatic attribution for deep networks. In *International conference on machine learning*, pp. 3319–3328. PMLR, 2017.
- Maria Tsimpoukelli, Jacob L Menick, Serkan Cabi, SM Eslami, Oriol Vinyals, and Felix Hill. Multimodal few-shot learning with frozen language models. *Advances in Neural Information Processing Systems*, 34:200–212, 2021.
- Ashish Vaswani, Noam Shazeer, Niki Parmar, Jakob Uszkoreit, Llion Jones, Aidan N Gomez, Lukasz Kaiser, and Illia Polosukhin. Attention is all you need. *Advances in neural information processing systems*, 30, 2017.
- Martina G Vilas, Timothy Schaumlöffel, and Gemma Roig. Analyzing vision transformers for image classification in class embedding space. In *Thirty-seventh Conference on Neural Information Processing Systems*, 2023.
- Kevin Ro Wang, Alexandre Variengien, Arthur Conmy, Buck Shlegeris, and Jacob Steinhardt. Interpretability in the wild: a circuit for indirect object identification in gpt-2 small. In *The Eleventh International Conference on Learning Representations*, 2023.
- Peng Wang, Shuai Bai, Sinan Tan, Shijie Wang, Zhihao Fan, Jinze Bai, Keqin Chen, Xuejing Liu, Jialin Wang, Wenbin Ge, et al. Qwen2-vl: Enhancing vision-language model’s perception of the world at any resolution. *arXiv preprint arXiv:2409.12191*, 2024.
- Chris Wendler, Veniamin Veselovsky, Giovanni Monea, and Robert West. Do llamas work in English? on the latent language of multilingual transformers. In Lun-Wei Ku, Andre Martins, and Vivek Srikumar (eds.), *Proceedings of the 62nd Annual Meeting of the Association for Computational Linguistics (Volume 1: Long Papers)*, pp. 15366–15394, Bangkok, Thailand, August 2024. Association for Computational Linguistics. doi: 10.18653/v1/2024.acl-long.820. URL <https://aclanthology.org/2024.acl-long.820>.
- Zhaofeng Wu, Xinyan Velocity Yu, Dani Yogatama, Jiasen Lu, and Yoon Kim. The semantic hub hypothesis: Language models share semantic representations across languages and modalities, 2024. URL <https://arxiv.org/abs/2411.04986>.
- Yuhui Zhang, Alyssa Unell, Xiaohan Wang, Dhruva Ghosh, Yuchang Su, Ludwig Schmidt, and Serena Yeung-Levy. Why are visually-grounded language models bad at image classification? *arXiv preprint arXiv:2405.18415*, 2024.

A FILTERED DATASET EXAMPLES



Figure 4: Example of dataset images for the object identification tasks.

B CURATED IMAGES AND QUESTIONS EXAMPLES



(a) “What is on the bench? It is a” → book



(b) “What is below the street sign? It is a” → bottle



(c) “What is on the truck? It is a” → dog



(d) “What is on the seat? It is a” → cup

Figure 5: Examples of curated images and their questions. We ask the model the question and prefill its answer with “It is a”. The correct answer is underlined.

C OBJECT CORRESPONDENCES

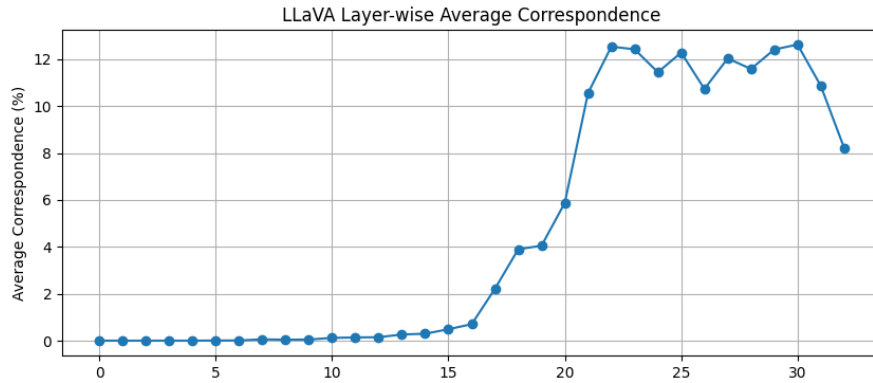


Figure 6: Token-to-object correspondence in LLaVA-1.5 across transformer layers. Analysis of 170 COCO images shows peak correspondence (23.7%) occurs in later layers (average layer 25.7/33).

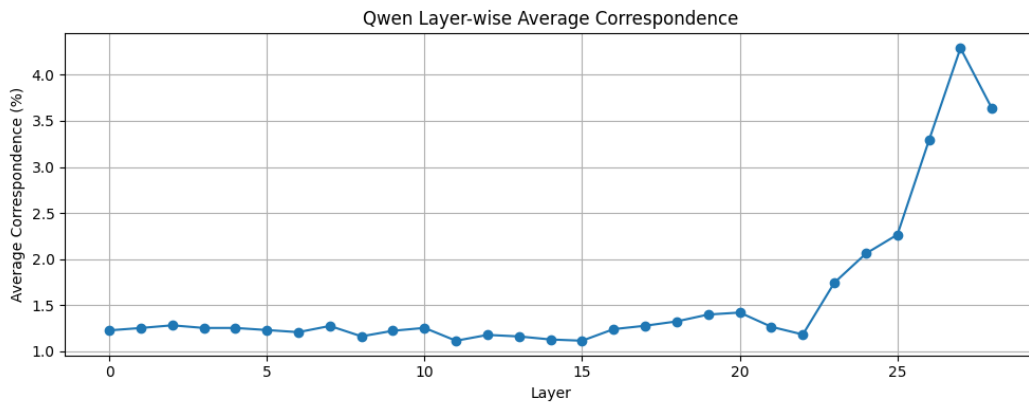


Figure 7: Token-to-object correspondence in Qwen2VL-2B showing increasing alignment in deeper layers, peaking at layer 25.1/29 with 6.5% correct mapping. Unlike LLaVA, Qwen exhibits non-zero correspondence in early layers.

D LLaVA-PHI-3 BLOCKING

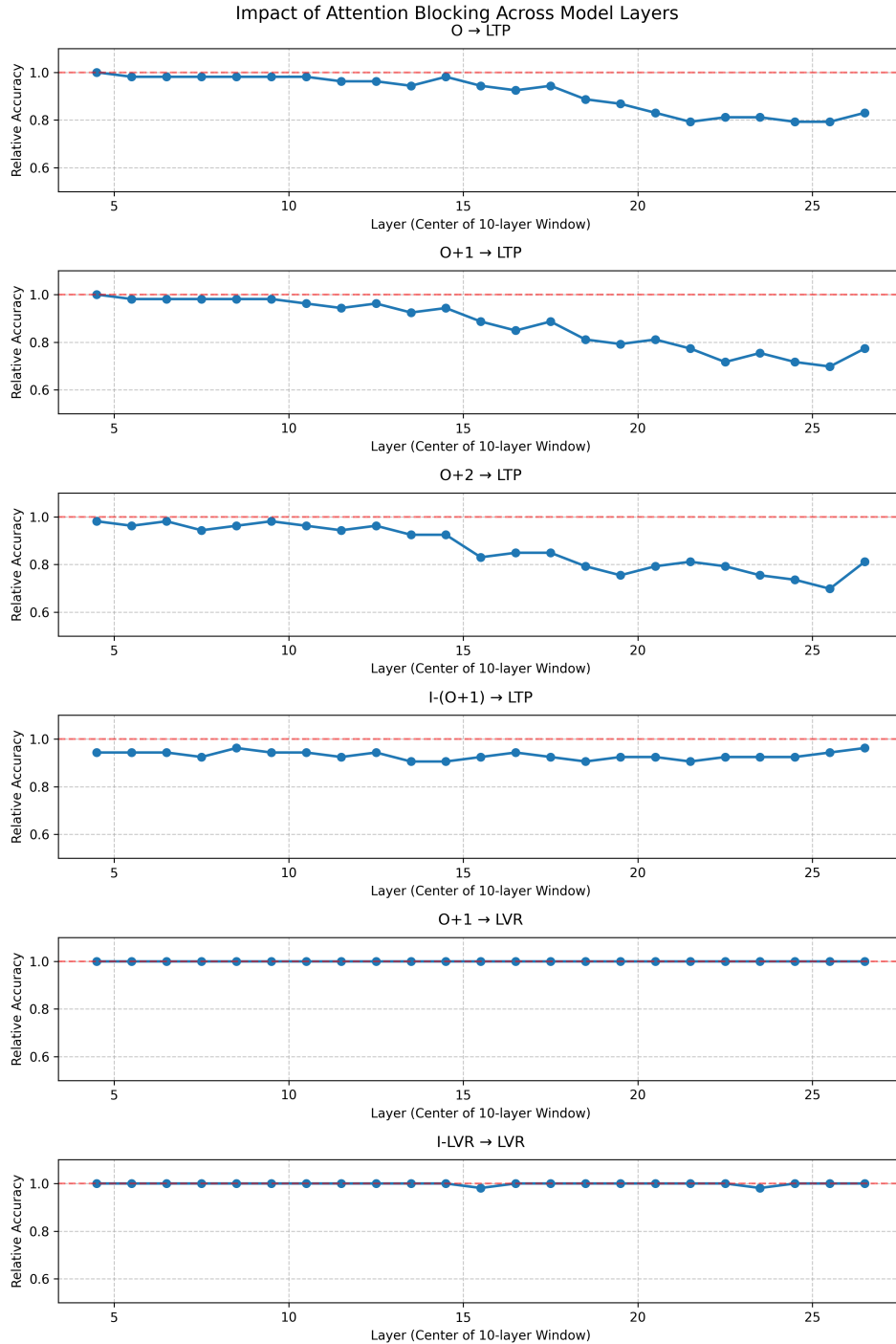


Figure 8: Attention blocking results for LLaVA-Phi-3 using a sliding window of 10 layers. We find that similar to LLaVA-1.5, blocking attention from object tokens to the last token position has the strongest effect in middle-to-late layers, while blocking attention from visual tokens to the last visual row shows minimal impact throughout the network.